Available online at www.sciencedirect.com
ScienceDirect
Ceramics International 33 (2007) 1469–1473
CERAMICS INTERNATIONAL
www.elsevier.com/locate/ceramint

Effect of dopants on the properties of metal-doped zirconia prepared by the glycothermal method

Jantana Wiwattanapongpan [a], Okorn Mekasuwandumrong [b], Choowong Chaisuk [b], Piyasan Praserthdam [a,*]

[a] *Center of Excellence on Catalysis and Catalytic Reaction Engineering, Department of Chemical Engineering, Faculty of Engineering, Chulalongkorn University, Bangkok 10330, Thailand*

[b] *Department of Chemical Engineering, Faculty of Engineering and Industrial Technology, Silpakorn University, Nakornpathom, Thailand*

Received 10 October 2005; received in revised form 22 March 2006; accepted 12 May 2006
Available online 29 September 2006

Abstract

The effects of dopants on zirconia prepared via the glycothermal method were investigated by XRD to determine the crystal structure and crystallite size. Morphologies of products were observed by SEM. The basic sites of zirconia were studied by CO_2-temperature programmed desorption (CO_2-TPD). The functional group in the samples was determined using IR. The intensity of Zr^{3+}, characterized by ESR, could be described as the oxygen coordinatively unsaturated Zr sites. The results suggest that doping elements can modify the surface chemistry of ZrO_2 to form hydroxyl groups and surface energies depending on the structure (cubic, tetragonal) in different dense phase. ESR peaks of Pb- and Bi-doped zirconia are different from the others, which showed high intensity of Zr^{3+}.

Keywords: Zirconia; Dopants; Nanocrystals; Glycothermal

1. Introduction

Zirconia is well known in different areas of chemistry such as in ceramics and catalysis because of its good mechanical, chemical and electrolytic properties. Its catalytic properties are especially promising because the zirconia surface contains both acidic and basic sites. It shows high activity and selectivity in many reactions [1–4].

Several dopants (yttria, ceria, magnesia, calcia, etc.) are usually added to stabilize the high temperature tetragonal and/or cubic phases [4]. If non-oxidizable impurities are dissolved into the cation sublattice, their presence may influence the defect formation energies of intrinsic defects, and/or lead to the formation of new associations [5]. Zirconia-doped with a lower valent cation has been highlighted as a good oxygen ion conductor, enhancing ionic conductivity and electrolytic stability [6]. The hydroxyl groups and the cationic and anionic defects in the structure certainly play an important role in catalytic properties [7]. The phase is influenced by composition, temperature, chemical composition (presence of additives) and preparative conditions.

Many techniques have been applied for synthesis of doped zirconia, including sol–gel [8], plasma-chemical method [9] and solvothermal synthesis [10]. Kongwudthiti et al. [10,11] reported the synthesis of nanocrystalline zirconia and Si-doped zirconia by the glycothermal method. The zirconia exhibited the high BET surface area and thermal stability.

In this work, metal-doped nanocrystalline zirconia was prepared via the glycothermal method and the effects of dopant (Si, Al, P, Ga, Pb and Bi) on the physical and chemical properties of zirconia were investigated.

2. Experimental

2.1. Sample preparation

Metal (Si, Al, P, Ga, Pb and Bi)-doped nanocrystalline zirconia with molar ratio of dopant/Zr 0.02 was prepared via the glycothermal method. Mixtures of zirconium tetra-*n*-propoxide and dopant precursors at 0.02 molar ratios of each dopant (tetraethyl-ortho-silicate, aluminium isopropoxide, tetraethylphosphate, gallium (III) acetylacetonate, lead (IV) acetate and

* Corresponding author.
E-mail address: piyasan.p@chula.ac.th (P. Praserthdam).

0272-8842/$32.00
doi:10.1016/j.ceramint.2006.05.014

bismuth (III) acetate) were suspended in 100 ml of 1,4-butanediol in a test tube, which was then placed in a 300 ml autoclave. The gap between the test tube and the autoclave wall was filled with 30 ml of 1,4-butanediol. The autoclave was purged with nitrogen. The mixture was heated to 300 °C at a rate of 2.5 °C/min. The temperature was held constant at 300 °C for 2 h. After reaction, the autoclave was cooled and the resulting powder yield was repeatedly washed with methanol and subsequently dried in air. Finally, the yield was calcined in air at 400 °C for 2 h.

2.2. Powder characterization

X-ray powder diffraction was performed with a Siemens D5000 using nickel filtered Cu Kα radiation. XRD patterns were measured at room temperature to identify crystal structure and estimate the crystallite size from line broadening according to the Scherrer equation [10,11]. The morphology of secondary particle was observed by scanning electron microscopy (SEM; JSM-5410LV). CO_2-temperature programmed desorption (CO_2-TPD) was conducted to measure the surface basicity of samples. They were first treated in flowing He at 400 °C for 1 h to remove the surface impurities and subsequently saturated in a flowing atmosphere, 30 ml/min, of pure CO_2 at 100 °C for 1 h. After saturation, the temperature was increased from 100 to 400 °C at 10 °C/min. The amount of desorbed CO_2 was determined by integrating the areas under curve of the desorption profiles. The functional group of the samples was determined using infrared spectroscopy, Nicolet model Impact 400. A JES-RE2X model electron spin resonance spectroscopy (ESR) was used to measure the intensity of Zr^{3+}. Before measurement, the sample was dried at 120 °C overnight. A 0.05 g of sample was placed in a sample tube, which was sealed at atmospheric pressure and room temperature.

3. Results and discussion

XRD patterns of the samples are shown in Fig. 1. Metal-doped and undoped ZrO_2 with metal/Zr ratio of 0.02 consisted of nanocrystalline tetragonal zirconia without contamination of the other phases (amorphous or secondary phases) except for Bi-doped ZrO_2 showing some monoclinic phase. This suggests that Bi^{3+} ion has lower valency and larger size than Zr^{4+} ion (1.11 and 0.84 Å for eight coordination, respectively) leading to instability and reorganization of ZrO_2 at lower temperature; some tetragonal phase changes to be more thermodynamically stable monoclinic polymorph [12]. The ion sizes of dopants are arranged as follows: P < Si < Al < Ga < Zr < Pb < Bi (0.38, 0.4, 0.54, 0.62, 0.84, 0.94 and 1.17 Å, respectively) [13].

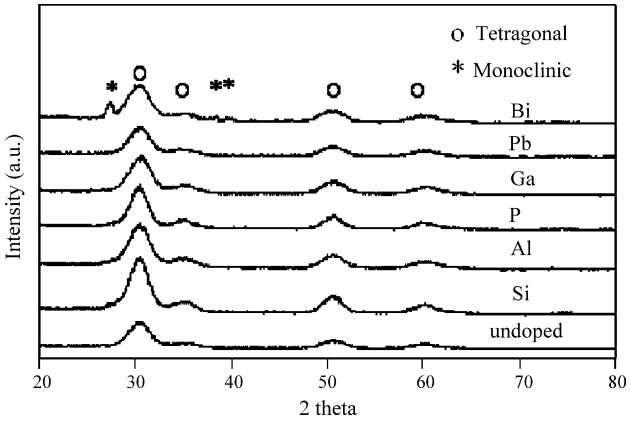

Fig. 1. The XRD patterns of undoped and doped ZrO_2 at 0.02 ratio of metal/Zr.

SEM micrographs of ZrO_2 and metal-doped ZrO_2 are shown in Fig. 2. Morphologies of pure and metal-doped ZrO_2 comprised spherical particles formed by aggregations of nanocrystalline primary particles. Doping with Si, Al, Ga and Bi at a ZrO_2 molar ratio of 0.02 has no effect on the spherical morphology of ZrO_2. Aggregation of microspheres and agglomeration of small aggregates were observed in SEM image for P-doped ZrO_2.

Table 1 summarizes the crystallite size and BET surface area of the products. Doping with Si, Al and P maintains the high BET surface area of ZrO_2, while Ga results in decreasing the BET surface area. On the other hand, the BET surface area ZrO_2 was significantly reduced by Pb and Bi doping; the decrease corresponded to the increased ionic size of the dopant ion. The crystallite sizes of samples were around 3–4 nm even after loading with any dopants. These indicate that the dopants affect the degree of agglomeration, but not the crystallization of ZrO_2. Pb- and Bi-doped ZrO_2 had high agglomeration of nanocrystalline ZrO_2. This prevents N_2 adsorption on the doped ZrO_2 surface and therefore decreases the BET surface area.

The formation of aggregates in solution can be examined by Derjaguin–Landua–Verwey–Overbeek (DLVO) theory, the energy barrier between two particles, which inhibit agglomeration, is expressed as follows [14]:

$$V_b = -\frac{A\kappa\alpha}{12} + 2\pi\varepsilon_o\varepsilon_r\alpha\phi^2$$

where A is the effective Hamaker constant, κ the Debye–Huckel parameter, α the particle diameter, ε_o the permittivity in the free space, ε_r the dielectric constant of the continuous phase and ϕ is the particle surface potential. Because the same solvent was used in all experiments, α, ε_o, ε_r and κ should be constant. According to the above equation, when dopants were introduced in the reaction system, the surface potential should be modified and this influences the aggregation level.

Fig. 3 shows the IR spectra of undoped and doped samples. The adsorption bands at around 600 cm^{-1} are assigned to

Table 1
Crystallite size, BET surface area, bulk density and amount of desorbed CO_2 of ZrO_2

Dopants	Crystallite size (nm)	Surface area (m^2/g)	Bulk density (g/cm^3)	Amount of CO_2 (μmol/g)
Undoped	3.6	114	1.02	27.6
Si	3.7	132	0.78	42.3
Al	3.2	121	1.24	63.9
P	4.1	138	0.88	52.7
Ga	3.1	87	1.44	26.4
Pb	3.3	2	1.43	0.0
Bi	3.1	34	1.33	22.6

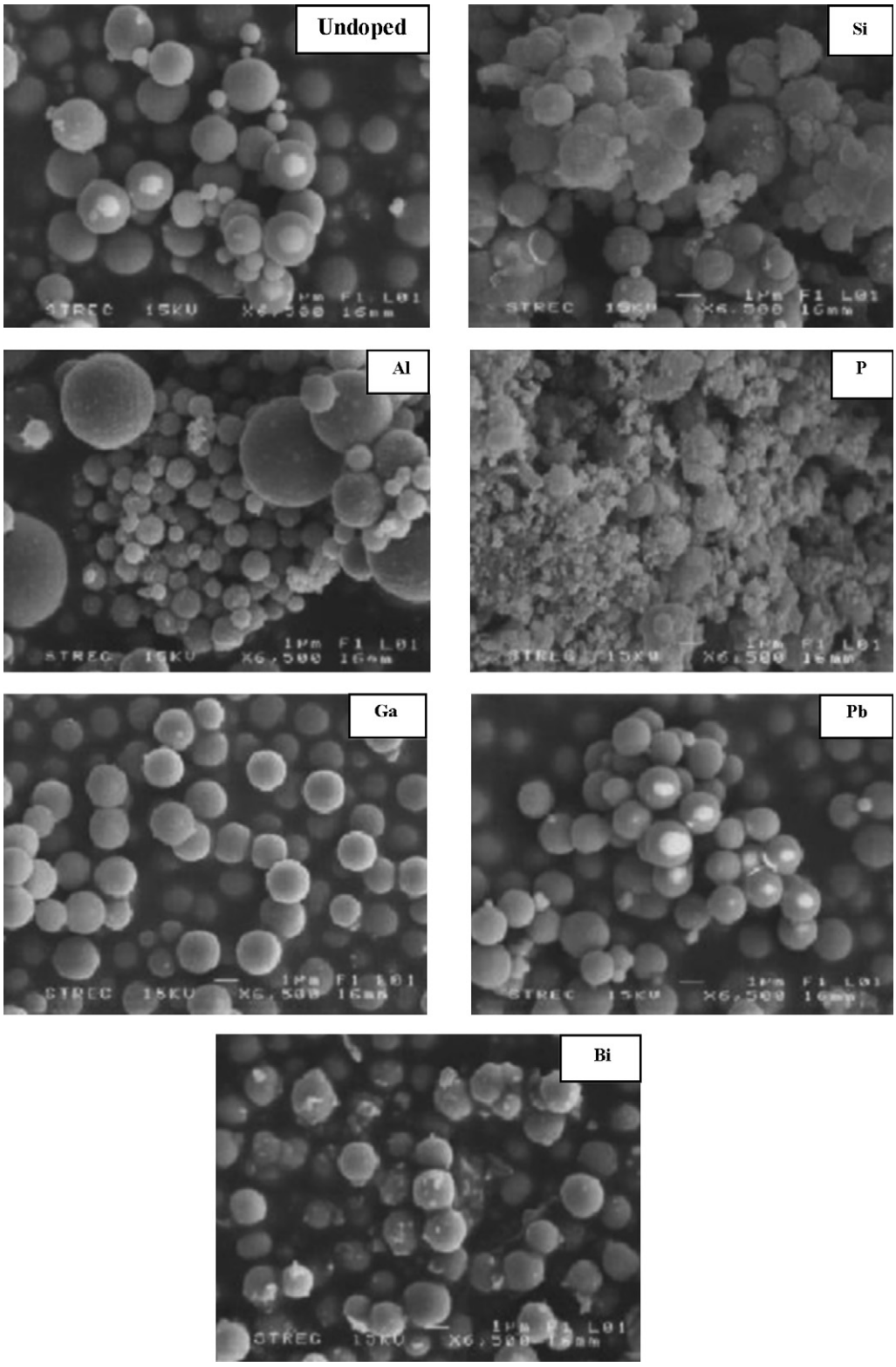

Fig. 2. SEM micrograph of undoped and doped ZrO_2 at 0.02 ratio of metal/Zr.

tetragonal zirconia. The band at ~1600 cm^{-1} is attributed to adsorbed water [15]. For Si doping, the bands at ~1000 cm^{-1} are attributed to Si–O–Zr bonds agreement with Kongwudthiti et al. [10,11]. This indicates that the Si atom incorporated into the zirconia lattice. The characteristic band of hydroxyl groups at around 3400 cm^{-1} [8,9] also appeared for all doped ZrO_2. However, a weak OH^- group can be observed for Pb- and Bi-doped ZrO_2. Cerrato et al. suggested that both non-dissociated H_2O molecules and OH species (dissociated H_2O) may contribute to the saturation of the coordinatively unsaturated

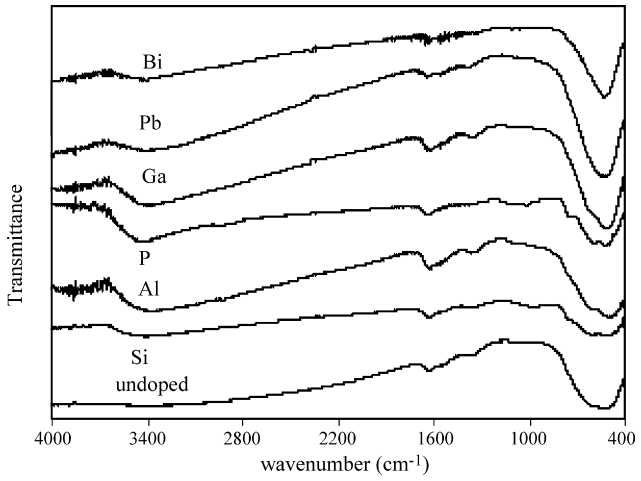

Fig. 3. IR spectra of undoped and doped ZrO_2 at 0.02 ratio of metal/Zr.

sites, which are cationic or anionic terminations produced in the outer layer of the solid [16]. These IR results indicate that adding dopants may modify surface chemistry to form hydroxyl groups.

The amounts of desorbed CO_2 were calculated from TPD thermograms and are shown in Table 1. Compared to the undoped ZrO_2, the desorbed CO_2 of Si-, Al- and P-doped ZrO_2 increased, while that of Ga-, Pb- and Bi-doped ZrO_2 decreased. The CO_2-TPD results are coincident with the BET surface area measurement in Table 1. Hence, the different amount of desorbed CO_2 should be due to differences in the BET surface area. However, the relationship between the BET surface area and the amount of desorbed CO_2 was not satisfied. This indicates that the amount of desorbed CO_2 depend not just on the BET surface area, but also on the presence of OH groups induced by doping with the other elements. Some authors mention that CO_2 was chemically bonded with the basic sites, oxygen vacancy sites and hydroxyl group over the metal oxide surface [16,17]. It has been reported that CO_2 adsorption over tetragonal zirconia surfaces can act as bidentate sites [18] and form bicarbonate groups by the interaction between OH groups and CO_2 [18,19]. In agreement with this adsorption behavior, pure zirconia with small amounts of OH groups detected by IR spectrum represented the amount of CO_2 desorbed less than doped zirconia. However, a large decrease on the BET surface area of Pb- and Bi-doped ZrO_2 occurred simultaneously the low amount of CO_2 desorbed. In addition, Wang et al. proposed that the surface basic sites might result from defect structures of metal oxide [20].

To identify defect centers of ZrO_2 assumed mainly to associate with Zr^{3+} sites, the spin of unpaired electrons was detected by mean of ESR. Correlation between relative ESR intensities and dopants is shown in Fig. 4. Zr^{3+} signals represented at $g_{\perp} \sim 1.97$ and $g_{||} \sim 1.95$ that was in good agreement with the position of Zr^{3+} observed by many researchers [21,22]. Bi- and Pb-doped ZrO_2 showed very sharp ESR peaks, which were assigned to Zr^{3+} due to oxygen vacancies. Hence, Zr^{4+} ions adjacent to oxygen vacancies may trap lone pair electrons resulting in formation of Zr^{3+}. This is agreement with Zhao et al. [23], who reported the formation of Zr^{3+} to be associated with the removal of hydroxyl group. For

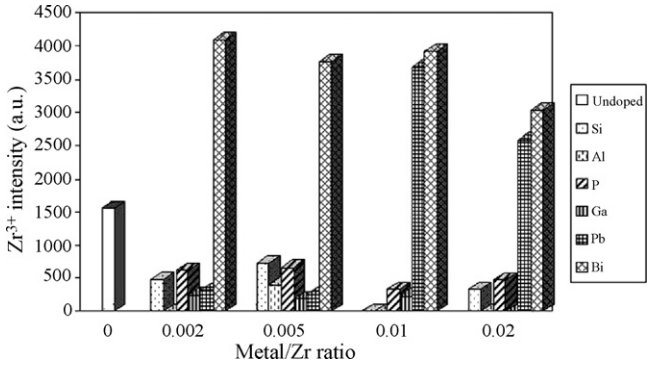

Fig. 4. Zr^{3+} intensity of undoped and doped ZrO_2 at 0.02 ratio of metal/Zr.

other dopants, decreasing Zr^{3+} intensity can be observed. It is attributed to the bonding of oxygen atom in OH group to the coordinatively unsaturated Zr sites.

From the above results, it was found that the small amounts of dopants influenced the properties of ZrO_2. Differences in the degree of aggregation (BET surface area), number of surface hydroxyl groups, CO_2 desorption and ESR intensities confirmed the modification effect resulting from dopants. The BET surface area, number of surface hydroxyl groups and CO_2 desorption can be improved by adding as the second element Si, Al, P and Ga which have the ionic sizes smaller than Zr^{4+} ion. However, the intensity of Zr^{3+} was in contrast with the presence of OH group. On the other hand, when zirconia was doped with larger ionic sizes (Pb and Bi), the existence of hydroxyl group correlated to the amount of desorbed CO_2 was decreased because of very low BET surface area arising from more aggregation in zirconia particles.

4. Conclusion

Metal (Si, Al, P, Ga, Pb and Bi)-doped ZrO_2 was successfully prepared via the glycothermal method. All samples were nanocrystalline tetragonal zirconia. The properties of ZrO_2 were modified and influenced by dopants ion sizes. The BET surface area increased after loading with Si, Al and P. While the BET surface area of Ga-, Pb- and Bi-doped ZrO_2 decreased. The hydroxyl groups were observed after loading with dopants due to the surface modification. ESR results showed increase of Zr^{3+} when either Bi or Pb was loaded. It seems the lager ionic size of dopants increased the amounts of Zr^{3+} and decreased BET surface area, hydroxyl groups and CO_2 desorption.

Acknowledgement

We would like to acknowledge financial supports from Commissions on Higher Education, Ministry of Education, Thailand.

References

[1] G. Li, W. Li, M. Zhang, K. Tao, Catal. Today 93–95 (2004) 595.
[2] B. Basa, J. Vleugels, O.V.D. Biest, Mater. Sci. Eng. A366 (2004) 338.
[3] J. Xue, J.H. Tinkler, R. Dieckmann, Solid State Ionics 166 (2004) 199.

[4] J.-H. Lee, S.M. Yoon, B.-K. Kim, J. Kim, H.-W. Lee, H.-S. Song, Solid State Ionics 144 (2001) 175.
[5] J.A. Wang, X. Bokhimi, A. Morales, O. Novaro, J. Phys. Chem. B 103 (1999) 299.
[6] V.S. Vladimir, W. Marcus, Chem. Mater. 15 (2003) 2668.
[7] M.M. Pineda, S. Castillo, T. Lopez, R. Gomez, C. Borboa, O. Novaro, Appl. Catal. B: Environ. 21 (1999) 79.
[8] X. Bokhimi, A. Morales, O. Novaro, M. Portilla, T. Lopez, F. Tzompantzi, R. Gomez, J. Solid State Chem. 135 (1998) 28.
[9] D. Das, H.K. Mishra, K.M. Parida, A.K. Dalai, J. Mol. Catal. A: Chem. 189 (2002) 271.
[10] S. Kongwudthiti, P. Praserthdam, W. Tanakulrungsank, M. Inoue, J. Mater. Process. Technol. 136 (2003) 186.
[11] S. Kongwudthiti, P. Praserthdam, M. Inoue, W. Tanakulrungsank, J. Mater. Sci. Lett. 21 (2002) 1461.
[12] C.R. Jagadish, R. Chitta, P. Panchanan, Mater. Lett. 58 (2004) 2140.
[13] G. Aylward, T. Findlay, SI Chemical Data, fifth ed., pp. 6–13.
[14] R. Hogg, T.W. Healy, D.W. Fuerstenau, Trans. Faraday Soc. 62 (1966) 1638.
[15] D.A. Skoog, J.J. Leary, Principles of Instrumental Analysis, Saundres College Publishing, Philadelphia, San Diego.
[16] G. Cerrato, S. Bordiga, S. Babera, C. Morterra, Appl. Surf. Sci. 115 (1997) 53.
[17] D. Anatoli, Molecular Spectroscopy of Oxide Catalyst Surface, John Wiley & Sons Ltd., Chichester, UK, 2003.
[18] M.E. Mariquez, T. Lopez, R. Gomez, J. Navarete, J. Mol. Catal. A: Chem. 220 (2004) 229.
[19] V.K. Diez, C.R. Apesteguia, J. Dicosimo, J. Catal. 215 (2003) 220.
[20] J.A. Wang, M.A. Valenzuela, X. Bokhimi, Colloids Surf. A: Physicochem. Eng. Aspects 179 (2001) 221.
[21] C. Morterra, E. Giamello, L. Orio, M. Volante, J. Phys. Chem. 94 (1990) 3111.
[22] H. Liu, L. Feng, X. Chang, Q. Xue, J. Phys. Chem. 99 (1995) 332.
[23] Q. Zhao, X. Wang, T. Cai, Appl. Surf. Sci. 225 (2004) 7.